Decreased Skp2 Expression Is Necessary but Not Sufficient for Therapy-Induced Senescence in Prostate Cancer

Jonathan A. Ewald and David F. Jarrard

Department of Urology, University of Wisconsin School of Medicine and Public Health, Carbone Comprehensive Cancer Center, University of Wisconsin, Madison, WI

Abstract

Therapy-induced senescence (TIS), a cytostatic stress response in cancer cells, is induced inefficiently by current anticancer agents and radiation. The mechanisms that mediate TIS in cancer cells are not well defined. Herein, we characterize a robust senescence response both *in vitro* and *in vivo* to the quinone diaziquone (AZQ), previously identified in a high-throughput senescence-induction small-molecule screen. Using AZQ and several other agents that induce senescence, we screened a series of cyclin-dependent kinase inhibitors and found that $p27^{Kip1}$ was induced in all investigated prostate cancer cell lines. The ubiquitin-ligase Skp2 negatively regulates $p27^{Kip1}$ and, during TIS, is translocated to the cytoplasm before its expression is decreased in senescent cells. Overexpression of Skp2 blocks the effects of AZQ on senescence and $p27^{Kip1}$ induction. We also find that stable long-term short hairpin RNA knockdown of Skp2 decreases proliferation but does not generate the complete senescence phenotype. We conclude that Skp2 participates in regulating TIS but, alone, is insufficient to induce senescence in cancer cells.

Translational Oncology (2012) 5, 278–287

Introduction

Accelerated or induced senescence is a regulated cellular response to sublethal stress wherein cells develop a permanently growth-arrested phenotype with distinct morphologic and biochemical characteristics [1–3]. These features include development of a flattened and enlarged morphology *in vitro* and increased senescence-associated β-galactosidase (SA-β-gal) activity in both cells and tissues [4]. Other characteristics of senescence have been used as surrogate markers including DNA damage and damage response signaling activities [5–7], secreted signaling factors [8], and other marker genes including *Maspin* and *Cspg2* [9,10]. Increased expression of one or more cyclin-dependent kinase inhibitor (CDKI) proteins, including $p16^{Ink4a}$ and $p21^{Waf1/Cip1}$, is critical to senescence [11]. In fibroblast-derived cell lines, transient expression of $p16^{Ink4a}$ or $p21^{Waf1/Cip1}$ induces senescence [7,12]. Deregulated CDKI expression contributes to senescence bypass and oncogenic transformation [3,11]. As the regulation of many of these pathways is affected in cancer, the contribution of CDKI protein regulation to therapy-induced senescence (TIS) of cancer cells remains undefined.

TIS occurs in tumors in response to radiotherapy or selected chemotherapy agents and is a potential strategy for cancer treatment [13,14]. Subtoxic doses of DNA damaging drugs induce senescence in cancer cells *in vitro*, including cells lacking p53 and other tumor suppressors [9,15,16]. Importantly, senescence has been observed, albeit infre-

quently, in patient tumors removed after treatment with genotoxic anticancer agents [17,18]. In cancer cells, senescence seems to have a neutral or antiproliferative effect on surrounding bystander cells [19,20]. *In vivo*, senescence induced genetically in tumor models results in immune-related tumor regression and extended survival [21,22]. Recently, senescence in colorectal cancer patients correlated with longer tumor-free survival after 5-fluorouracil/leucovorin treatment [23]. In all, accumulating evidence suggests that senescence in tumor tissues may prove to be a beneficial response to therapy.

TIS has not been widely studied in tumor models owing to a lack of effective compounds specifically inducing this phenotype. We recently identified diaziquone (AZQ) in a high-throughput screen for senescence-inducing drugs [24]. This compound is a rationally designed DNA-alkylating compound previously developed as an anticancer agent [25]. These early investigations focused on the extent that AZQ induced tumor cell death and did not take into account the possibility of tumor cell senescence as a response to treatment.

Address all correspondence to: David F. Jarrard, MD, 7048 WIMR, 1100 Highland Ave, Madison, WI 53705-2275. E-mail: jarrard@surgery.wisc.edu

Skp2 and p27^{Kip1} mediate the development of prostate intra-epithelial neoplasia and characteristics of the senescent phenotype [26]. The E$_3$-ubiquitin ligase Skp2 is central to the control of a number of important cancer-related processes. Skp2 is an F-box protein that regulates the specificity of ubiquitin-conjugating protein complexes, resulting in ubiquitination and subsequent degradation of a repertoire of targeted proteins [27]. Skp2 negatively regulates the expression of the CDKI p27^{Kip1}, with increased Skp2 expression decreasing p27^{Kip1} and resulting in proliferation. In prostate and other cancers, elevated Skp2 expression predicts poor prognosis [28,29] and is regulated by pathways affecting prostate carcinogenesis, including androgen receptor signaling [30] and the phosphoinositide 3-kinase/PTEN/Akt pathway [31–33]. Skp2 expression is also regulated by other pathways, including Cks1, anaphase-promoting complex/cyclosome, and the Forkhead-related transcription factor FOXM1 [27,34,35]. Although this body of evidence demonstrates the importance of Skp2 and p27^{Kip1} in regulating proliferation, the role of these proteins in TIS of cancer cells has not been addressed.

In the current study, we characterize senescence induction using AZQ and other compounds to investigate a novel role for Skp2 and p27^{Kip1} in the regulation of TIS. We find that while Skp2 is required for the induction of TIS, its down-regulation alone is insufficient to induce senescence.

Materials and Methods

Cell Lines and Reagents

DU145, PC3, and LNCaP cells were cultured as previously described [16,20]. AZQ (NSC 182986) was provided by the Developmental Therapeutics Program, Division of Cancer Treatment and Diagnosis, National Cancer Institute, National Institutes of Health (Bethesda, MD). Chemical information was obtained from PubChem (www.ncbi.nlm.nih.gov/sites/entrez). Doxorubicin and 5-azacytidine (5-AZA) were purchased from Sigma (St Louis, MO).

Viable Cell Counting, Side Scatter, and Cell Cycle Modeling

DU145 and PC3 cells were plated in six-well plates at a density of 50,000 cells per well and LNCaP cells plated at a density of 200,000 cells per well. After overnight incubation, cells in sample wells were collected and stained with Annexin V–Alexa 488 and propidium iodide (PI; Invitrogen, Carlsbad, CA). The fraction and number of viable cells in each sample was measured by flow cytometry and calculated as previously described [20]. Simultaneously, the cellular granularity of viable cells in each sample was measured as side scatter (SSC). Parallel samples were then cultured for 3 days in medium containing 250 nM AZQ before counting or were cultured in 250 nM AZQ for 3 days followed by washing in phosphate-buffered saline (PBS) and three additional days of culture in drug-free medium before they were collected and counted. Flow cytometry data were analyzed using WinMDI (Joseph Trotter, Scripps Research Institute, La Jolla, CA). In addition, parallel samples cultured and treated on glass cover slips were fixed and stained for SA-β-gal activity as previously described [4] and visualized by light microscopy. For cell cycle modeling, cells were collected and stained using PI, and cellular DNA content was measured by flow cytometry as previously described [20,36]. The cell cycle phase was estimated using Cylchred by Terry Hoy of University of Wales College of Medicine (Cardiff, United Kingdom).

DU145 Xenograft Tumors

Animal protocols and studies were performed in accordance with the guidelines of the Association for the Assessment and Accreditation of Laboratory Animal Care International, and approval was obtained from the University of Wisconsin Institutional Animal Care and Use Committee. Male athymic nude mice were purchased from Harlan (Madison, WI), and xenograft tumors were established and measured as previously described [20,37]. When tumors reached measurable size (1 mm^3), mice were given intraperitoneal injections of PBS or 4 mg of AZQ per kilogram body weight three times a week for 3 weeks. This dosage is approximately half the reported maximum tolerable dose in mice [25]. Tumor size was monitored until exceeding 1200 mm^3, at which time tumors were harvested; tumors that had not exceeded this size were harvested 15 weeks after tumors were initially detected. Tumor samples were frozen in a sectioning medium or fixed in paraformaldehyde and embedded in paraffin. Sections of frozen tumors were stained for SA-β-gal activity as previously described [4]. Additional DU145 xenograft tumors were administered single doses of PBS or AZQ, harvested 7 days later, and frozen or fixed and embedded, as mentioned previously.

Immunohistochemistry

Collected tissues were fixed for 24 hours in 10% neutral buffered formalin, dehydrated, paraffin infiltrated, and paraffin embedded. Tissue sections were cut at 5 μm and mounted on slides. Sections were deparaffinized in xylene, hydrated through graded ethyl alcohols to water, washed with PBS, subjected to antigen retrieval, and blocked with 10% goat serum in PBS. Endogenous peroxidase was blocked with 0.3% hydrogen peroxide in methanol. Endogenous biotin was blocked with 0.001% avidin in PBS and quenched with 0.001% biotin in PBS. Sections were then incubated with primary antibody at a 1:25 dilution in PBS with 1% goat serum overnight at 4°C, washed with PBS, and incubated with biotinylated goat anti-rabbit or antimouse secondary antibodies (Vector Laboratories, Burlingame, CA) at 1:200 in PBS at room temperature. Slides were washed in PBS, incubated at room temperature with Vectastain ABC Elite (Vector Laboratories), washed in PBS, developed with diaminobenzidine (Vector Laboratories), and counterstained with Mayer hematoxylin. Stained sections were visualized by light microscopy. Primary antibodies: p27^{Kip1} (no. 610242; BD Biosciences, Lexington, KY), Ki-67 (VP-K452; Vector Laboratories, Inc), and cleaved caspase 3 (no. 9661; Cell Signaling Technology, Beverly, MA).

Cell Lysates and Protein Immunoblot Analysis

DU145, PC3, and LNCaP cells were cultured in growth medium or medium containing 250 nM AZQ for 3 days, and cells were exposed to AZQ followed by 3 days in drug-free medium, washed with warm PBS, scraped from culture plates, collected, pelleted, and solubilized in lysis buffer (PBS containing 2% NP-40, 10 mM NaF, 1 mM Na$_4$VO$_3$, 10 μg/ml aprotinin, 10 μg/ml leupeptin), removing insoluble debris by centrifugation. Equal amounts of total cell protein in each lysate were separated by SDS-PAGE in 4% to 12% Bis/Tris gradient gels (Invitrogen) and transferred to nitrocellulose membranes. Membranes were blocked and probed with antibodies, as previously described [36,38].

In additional experiments, DU145 and PC3 cells were cultured in 250 nM AZQ (as above), 25 nM doxorubicin, or 400 nM 5-AZA, as previously described [16]. Cells were solubilized in lysis buffer after 2 and 3 days in medium containing each respective drug or after 3 days in drug-containing medium plus 3 days of culture in drug-free medium. Antibodies were as follows: p15^{Ink4b} (sc-613), p16^{Ink4a} (sc-468),

p21$^{Waf1/Cip1}$ (sc-397), p27^{Kip1} (sc-528), p57^{Kip2} (sc-1040), and Skp2 (sc-7164; Santa Cruz Biotechnology, Santa Cruz, CA); α-tubulin (CP06; Calbiochem, San Diego, CA); HRP-conjugated anti-mouse and anti-rabbit secondary antibodies (nos. 31432 and 31464; Thermo/Pierce, Rockford, IL). Band intensities were measured using ImageJ (http://rsbweb.nih.gov/ij/), background intensities were subtracted and normalized to α-tubulin intensities and expressed in relative units as a function of control band intensity. In each case, the immunoblot presented is representative of at least three experiments.

Immunofluorescence of p27^{Kip1} and Skp2

PC3 cells were plated on glass cover slips. Control proliferating cells or cells treated with 250 nM AZQ for 2, 3, or 3 days plus three additional days in drug-free medium were fixed in paraformaldehyde and stained as previously described [33] using antibodies recognizing p27^{Kip1} (BD Biosciences) and Skp2 (Santa Cruz), with Alexa 488 or Alexa 594–conjugated secondary antibodies (Invitrogen). Nuclei were stained using Hoechst 33342 (Invitrogen). Cells and tissues were visualized using fluorescence microscopy as previously described [20,39].

Skp2 Expression and Effects on Proliferation

The complementary DNA (cDNA) for Skp2 was purchased from Open BioSystems (no. IHS1380-97652024; Huntsville, AL) and subcloned into the pCDNA3.1(+) expression vector (Invitrogen) where the cDNA sequence was confirmed. Equal amounts of Skp2-pCDNA3.1 and pSico-PGK-GFP (Addgene, Cambridge, MA) were coelectroporated into DU145 and PC3 cells using the Amaxa Nucleofector System and reagents (Lonza, Basel, Switzerland). Control samples were transfected with a pCDNA3.1 vector containing the LacZ cDNA. After electroporation, cells were incubated overnight in growth medium, and medium was replaced with drug-free medium or medium containing 250 nM AZQ and cultured for two additional days. Samples were solubilized in lysis buffer, and expressions of Skp2, p27^{Kip1}, and α-tubulin were assessed by immunoblot analysis, as mentioned previously. In parallel samples, nonfixed cells were collected and suspended in PBS containing both 50 μg/ml PI (to identify viable cells) and 10 μg/ml Hoechst 33342 (to assess DNA content), as previously described [40]. Samples were analyzed by flow cytometry using an LSR-II flow cytometer (Becton-Dickinson, Franklin Lakes, NJ) to measure DNA content in viable, green fluorescent protein (GFP)–coexpressing cells. Cellular DNA content data were analyzed as previously mentioned.

Conditional Expression of Skp2 Short Hairpin RNA

To ablate p53 function in LNCaP cells, cells were infected with retrovirus containing the human papillomavirus type 16 E6 protein and selected with 500 μg/ml G418 [38,41]. LNCaP, LNCaP + E6, and DU145 were transduced with lentivirus containing either control or Skp2-specific short hairpin RNA (shRNA) in the pTRIPZ vector (nos. 199552 and 12473; Open Biosystems) according to the manufacturer's protocols and selected with 1 μg/ml puromycin to generate cell lines stably harboring this vector. The expression of multiple Skp2-targeting shRNAs similarly decreased Skp2 protein expression, and one construct (no. 199552) was used for the remainder of the experiments. The expression of control shRNA did not affect Skp2 expression or proliferation (not shown). Cells were cultured in 2 μg/ml doxycycline (Sigma) for 7 days and for 7 days with seven additional days ± 2 μg/ml doxycycline. Cells were lysed for Western blot analysis of protein expression and were assessed for proliferation by DNA staining.

Statistical Methods

Data were analyzed, SE was calculated, and Student's *t* test was performed using Excel (Microsoft Corp, Redmond, WA). Error bars in all figures represent SE. Analysis of variance (ANOVA) was performed to determine whether the sizes of control and AZQ-treated xenograft tumors were significantly different. The Kaplan-Meier estimator was used to determine whether survival of control or AZQ-treated tumors was significantly different using a tumor volume of 1200 mm^3 as a surrogate for mortality.

Results

Characterization of Senescence Induction by AZQ in Prostate Cancer In Vitro and in Xenograft Tumors

The DNA-alkylating drug AZQ (Figure 1A) was recently identified in a drug screen designed to identify senescence in immortalized cancer cells by our group [24]. We performed dose-ranging studies and found that 250 to 500 nM AZQ significantly induced senescence in advanced prostate cancer cell lines DU145, PC3, and LNCaP cells based on SA-β-gal staining and morphology (Figure 1B). Detection of apoptosis by Annexin V and propidium iodide staining 3 days after AZQ exposure revealed cell viability similar to that of controls (Table 1) and a significant increase in SSC, a measurement of cellular complexity that is increased in senescent cells [14] (Table 1). Moreover, a significant percentage of cells accumulated in the G$_2$/M phase after AZQ exposure, suggesting reduced proliferation and growth arrest (Table 1). These initial results had suggested the possibility that AZQ induces cellular senescence in these cancer cell lines.

By definition, senescent cells are viable but persistently growth arrested, even after the addition of mitogens [42]. To demonstrate that AZQ induces a growth arrest that persists after drug removal, prostate cancer cell lines were cultured with and without 250 nM AZQ for 3 days. Cell numbers were consistently lower in drug-treated samples, and this growth inhibition persisted after further culture in drug-free medium (Figure 1C). Furthermore, after drug removal and 2 weeks in drug-free medium, AZQ-treated DU145, PC3, and LNCaP cells remained nonproliferative with senescence-like morphology, although recovered proliferation of many DU145 cells was apparent (not shown). These results demonstrate that exposure to AZQ efficiently induces senescence in a variety of prostate cancer cell lines.

To determine whether AZQ has antiproliferative effects on prostate tumors *in vivo*, DU145 xenograft tumors were established in athymic nude mice and treated with 40% of the maximum tolerated AZQ dose in mice (10 mg/kg) [25]. Animals with established tumors were treated for 3 weeks with AZQ (three doses per week) or dimethyl sulfoxide (DMSO). Tumor growth in AZQ-treated mice was significantly decreased and remained largely unchanged until 9 weeks after the initial treatment, with no effect on animal weight (Figure 2A; ANOVA least squares, *P* < .005). Tumors in control mice grew rapidly to 1200 mm^3 within 7 weeks, at which point animals were killed. Survival was significantly prolonged in AZQ-treated tumors (Figure 2B; log-rank, *P* < .008). Growth in xenografts injected with only one or three total doses of AZQ was not significantly affected (not shown).

Samples of harvested tumors were separately frozen in sectioning medium or were formalin-fixed and paraffin-embedded. Staining for SA-β-gal activity was increased in AZQ-treated tumors compared to that in controls (Figure 2C; Student's *t* test, *P* = .02). AZQ-treated tumors had decreased proliferation as assessed by Ki-67 quantitation (Figure 2D; Student's *t* test, *P* = .034). The apoptosis marker cleaved
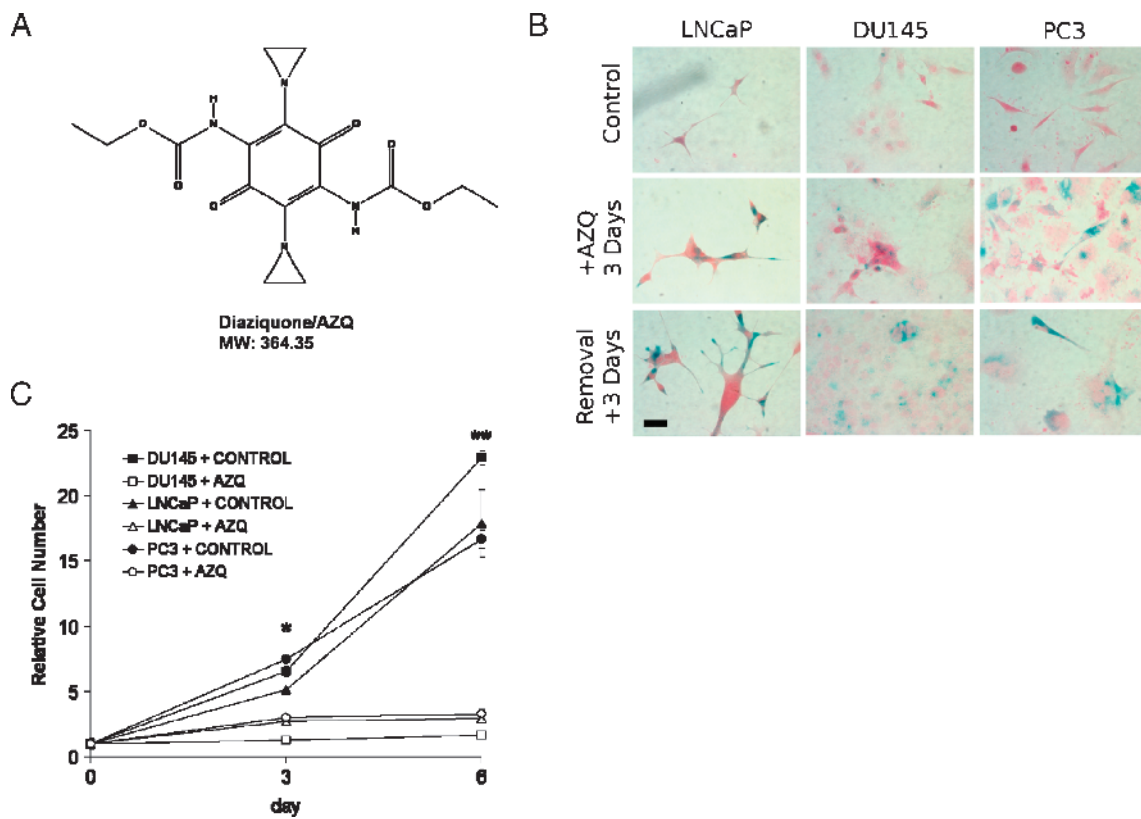
Figure 1. AZQ induces senescence in prostate cancer cells *in vitro*. (A) Structure and molecular weight of AZQ (NSC 182986). (B) Morphology and SA-β-gal staining of control DU145, PC3, and LNCaP cells and after 3 days cultured with medium containing 250 nM AZQ and with additional 3 days of recovery in drug-free medium. Scale bar, 20 μm. (C) AZQ inhibits prostate cancer cell growth. Prostate cancer cells were cultured in medium + DMSO (Control) or in medium + 250 nM AZQ for 3 days and then cultured for three additional days in drug-free medium to day 6 (+ AZQ). Viable cell number was measured as described in Materials and Methods. Student's *t* test, *$P < .02$, **$P < .01$.

caspase 3 was minimally detected and not significantly induced (not shown). In sum, these data demonstrate that prolonged administration of low-dose AZQ significantly limited tumor growth, prolonged survival, and induced characteristics of senescence in a prostate xenograft tumor model *in vivo*. Given the effectiveness of AZQ to induce senescence, we evaluated the mechanisms regulating this response.

Induction of the CDKI p27^Kip1 and Down-regulation of Skp2 in TIS

Although CDKI protein expression is central to senescence growth arrest in fibroblast and epithelial cells, CDKI regulation is frequently disrupted in cancers [38,42,43]. To identify CDKIs that are upregulated in TIS, prostate cancer cells were cultured for 3 days in medium containing 250 nM AZQ, and an additional 3 days in drug-free medium before protein lysates were harvested. Proteins were then analyzed by immunoblot using antibodies identifying the CDKI proteins p21$^{\text{Waf1/Cip1}}$ and p27$^{\text{Kip1}}$. We found that p27$^{\text{Kip1}}$ expression increases in all three cell lines after exposure to AZQ and drug-free medium, with a higher basal expression apparent in LNCaP cells (Figure 3A). The expression of p21$^{\text{Waf1/Cip1}}$ was not detected in DU145 and PC3 cells, and in LNCaP cells, the basal expression of p21$^{\text{Waf1/Cip1}}$ was elevated and affected by AZQ (Figure 3A). The expression of p57$^{\text{Kip2}}$, p16$^{\text{Ink4a}}$, and p15$^{\text{Ink4B}}$ was not detected in any of the three cell lines (data not shown). We then assessed the expression of p27$^{\text{Kip1}}$ in DU145 xenograft tumors harvested 7 days after a single intraperitoneal injection of 4 mg/kg AZQ ($n = 4$ each). Both nuclear and cytoplasmic p27$^{\text{Kip1}}$ expressions were

increased in AZQ-treated tumors compared with those in controls (Figure 3B). Treated tumors also extensively stained positively for SA-β-gal activity (Figure 2C). We find that p27$^{\text{Kip1}}$ is the only CDKI consistently induced in cell lines undergoing senescence growth arrest.

Table 1. Effect of AZQ on Viability, Cellular Granularity (SSC), and Cell Cycle in Prostate Cancer Cell Lines.

Cell Line	Measurement	Control	+AZQ
DU145	Normalized % viable cells	100 ± 1	75 ± 2*
	Normalized SSC	0 ± 5	46 ± 2*
	% G$_1$/G$_0$	43.1 ± 0.7	18.0 ± 1.2*
	% S	35.9 ± 0.5	16.7 ± 4.7*
	% G$_2$/M	21.0 ± 0.6	65.2 ± 3.8*
PC3	Normalized % viable cells	100 ± 1	96 ± 3
	Normalized SSC	0 ± 5	76 ± 5*
	% G$_1$/G$_0$	44.8 ± 2.0	19.1 ± 1.1*
	% S	33.0 ± 3.1	15.9 ± 1.1*
	% G$_2$/M	22.2 ± 1.9	65.0 ± 1.9*
LNCaP	Normalized % viable cells	100 ± 7	84 ± 8
	Normalized SSC	0 ± 6	131 ± 7*
	% G$_1$/G$_0$	69.0 ± 0.9	36.7 ± 0.9*
	% S	17.3 ± 2.1	21.2 ± 1.0
	% G$_2$/M	13.6 ± 1.7	42.1 ± 2.8*
All Data	Normalized % viable cells	100 ± 1	85 ± 3*
	Normalized SSC	0 ± 3	85 ± 13†
	% G$_1$/G$_0$	52.3 ± 8.4	24.6 ± 6.1†
	% S	28.7 ± 5.8	17.9 ± 1.7
	% G$_2$/M	19.0 ± 2.7	57.5 ± 1.7*

*$P < .01$, two-tailed equal variance Student's *t* test.
†$P < .05$, two-tailed equal variance Student's *t* test.

We next investigated whether expression of the $p27^{Kip1}$-regulator Skp2 is altered in AZQ-induced senescence. Initial experiments measuring mRNA expression showed no increase in $p27^{Kip1}$ transcription in DU145 or PC3 cells after AZQ (not shown). In contrast, in protein lysates of cells treated with 250 nM AZQ and allowed to recover in drug-free medium, the expression of Skp2 decreased compared to that in proliferating cells (Figure 4A). We addressed whether changes in Skp2 and $p27^{Kip1}$ expression were AZQ-specific or occurred in senescence induced by other drugs. Prostate cancer cells were cultured with AZQ and known senescence-inducing doses of the DNA-damaging anthracycline doxorubicin (DOX) or the DNA methyltransferase inhibitor 5-AZA [3,16]. Protein lysates were harvested at multiple time points after drug exposure and analyzed by immunoblot analysis. Skp2 expression was reduced at later time points after senescence-inducing drug contact consistent with induction of the senescent phenotype (Figure 4B). However, the increased expression of $p27^{Kip1}$ appeared earlier than decreased Skp2 in these time-course experiments, a point that will be experimentally addressed in later paragraphs. In summary, these data demonstrate that changes in $p27^{Kip1}$ and Skp2 expression constitute a consistent molecular change in prostate cancer cell lines exposed to senescence-inducing doses of various drugs.

Skp2 activity is regulated by nuclear/cytoplasmic localization in addition to expression [33]. We used immunofluorescence to determine whether changes in Skp2 localization that occur in TIS would explain the kinetics of $p27^{Kip1}$ and Skp2 expression (Figure 4B). In control cells, minimal $p27^{Kip1}$ is detected, whereas Skp2 expression is primarily localized in the nucleus of PC3 cells (Figure 4C). Early after exposure to AZQ (days 2 and 3), increased $p27^{Kip1}$ is detected and Skp2 expression is translocated from the nucleus to the cytoplasm. With development of the full senescent phenotype (observed in cells 6 days after initial drug exposure), nuclear expression of $p27^{Kip1}$ is increased and Skp2 expression decreased. These data indicate that Skp2 translocation from the nucleus to the cytoplasm is an early event that regulates $p27^{Kip1}$ accumulation during TIS.

Skp2 Regulates Growth Arrest in TIS

Skp2 regulates the expression of $p27^{Kip1}$ in numerous cell types, including prostate cells [27]. To determine the role Skp2 plays in
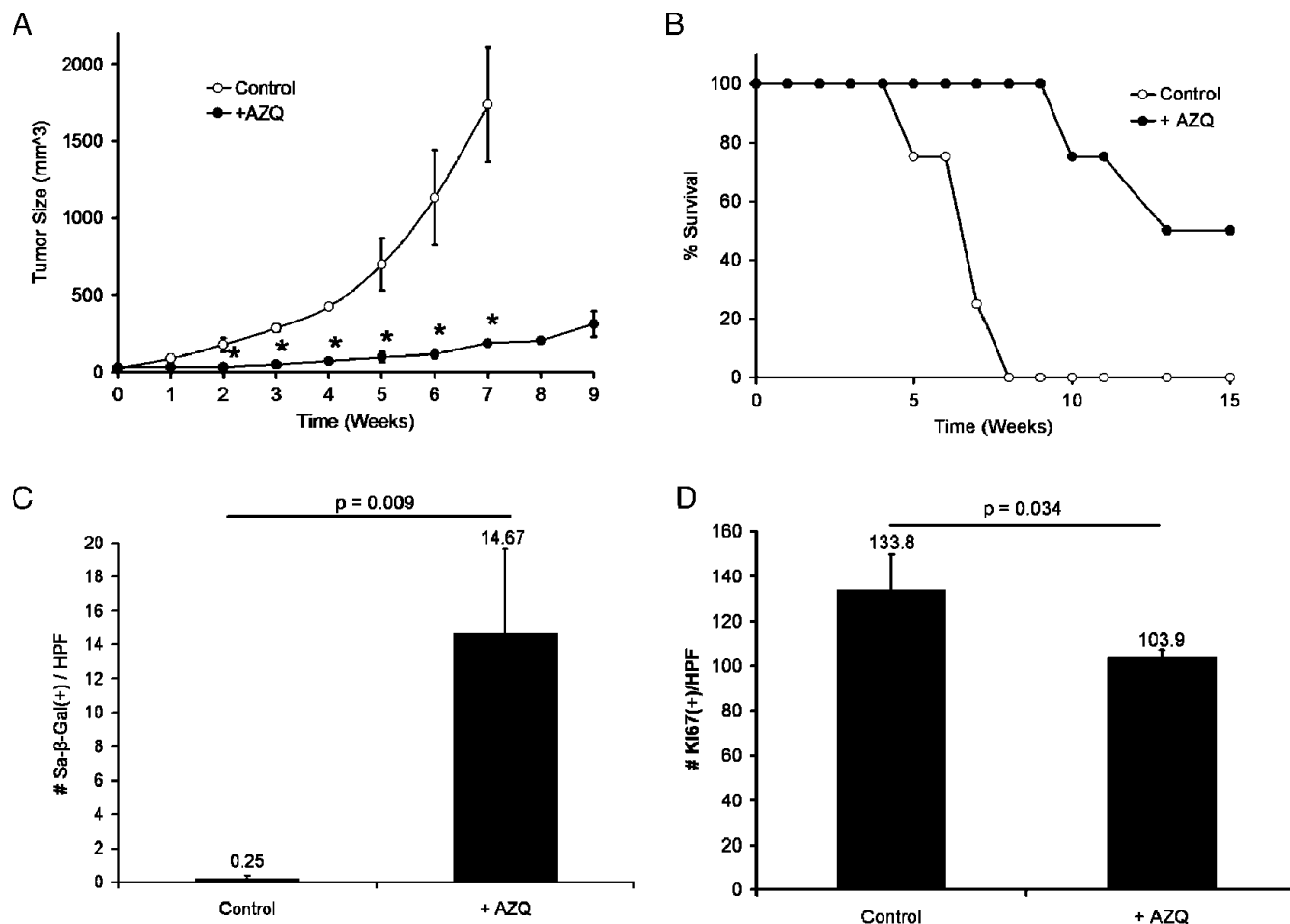

Figure 2. AZQ induces senescence growth arrest in DU145 xenograft tumors *in vivo*. After 3 weeks of growth to measurable size (week 0), tumor-bearing mice were given intraperitoneal injections of control DMSO in PBS or 4 mg of AZQ/kg body weight three times a week for 3 weeks ($n = 4$ for each). (A) Change in size of established DU145 xenograft tumors. Note the persistence of tumor growth inhibition after 3 weeks (*ANOVA, $P < .005$). (B) Kaplan-Meier analysis of time for Control or +AZQ tumors to reach study end point of 1200-mm^3 tumor volume (log rank, $P < .008$). (C) SA-β-gal staining is induced in AZQ-treated tumors compared with controls. These data represent the average number of positive staining cells per 400× high-power field in five views per tumor ($n = 4$ tumors each). Student's t test, $P = .009$. (D) Decreased expression of the proliferation marker Ki-67 in +AZQ tumors *versus* Control measured as in C. Student's t test, $P = .034$.
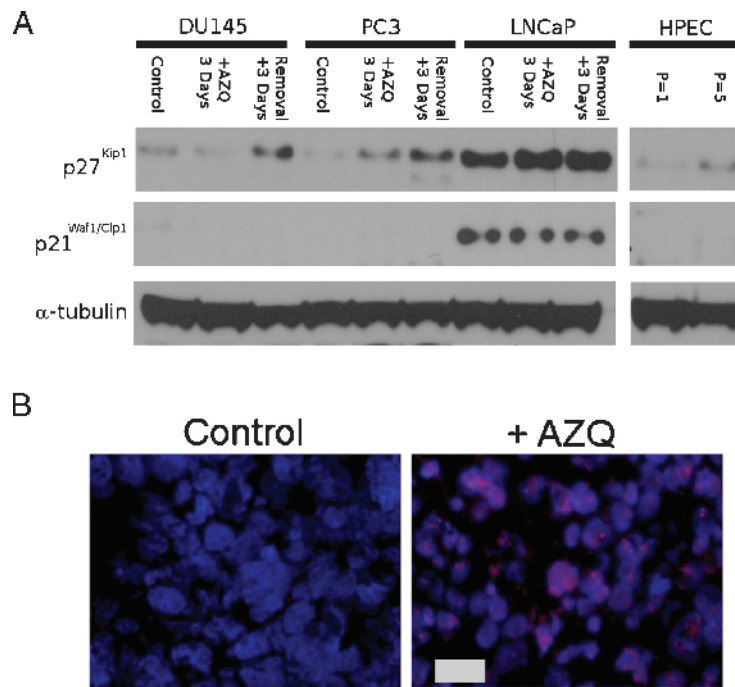
Figure 3. Increased expression of CDKI p27^{Kip1} in senescent prostate cancer cell lines *in vitro* and DU145 xenografts *in vivo* after AZQ treatment. (A) DU145, PC3, and LNCaP cells were cultured for 3 days in medium containing 250 nM AZQ (+AZQ 3 Days) or were exposed to AZQ and cultured an additional 3 days in drug-free medium (Removal + 3 Days), protein lysates were harvested. Lysates of nonconfluent proliferating cells were used as controls. Lysates of normal human prostate epithelial cells after one and five passages were included. Expression of α-tubulin was included as a loading control. Band intensities are normalized to α-tubulin and expressed relative to controls. (B) Immunofluorescence microscopy of p27^{Kip1} expression (red) in Control or +AZQ tumors harvested 7 days after a single injection of 4 mg of AZQ per kilogram body weight. DNA is stained using Hoechst 33342 (blue). Scale bar, 20 μm.

TIS, we first tested whether Skp2 overexpression could rescue the senescence-inducing effect of AZQ. Cells were coelectroporated with a plasmid expression vector containing the cDNA for Skp2 or control LacZ and a GFP expression vector to specifically monitor electroporated cells [40]. In preliminary experiments, transient overexpression of Skp2 persists 3 days after electroporation, after which expression decreases markedly (not shown). Therefore, cells were exposed to 250 nM AZQ 24 hours after electroporation and were assessed 2 days later. Cells were harvested and analyzed for protein expression by immunoblot analysis and for proliferation by flow cytometry (Figure 5A). In LacZ-expressing cells, AZQ exposure increased p27^{Kip1} expression and decreased the fraction of cells in the S phase, consistent with cellular senescence. In Skp2-overexpressing cells, p27^{Kip1} expression did not increase after AZQ exposure, and S phase was increased (Figure 5B). These results demonstrate that forced overexpression of Skp2 interrupts the response to AZQ indicating that decreased Skp2 is necessary for TIS growth arrest.

Previous studies have shown that the increased expression of p27^{Kip1} is associated with senescence in human prostatic intraepithelial neoplasia (PIN) and in cell lines [7,26]. We addressed whether reduced expression of Skp2 is sufficient to induce senescence in cancer cells. Stable prostate cancer cell lines derived from LNCaP, DU145, and LNCaP + E6 cells (expressing the p53-targeting human papillomavirus type 16 E6 protein) were developed to express Skp2 shRNA in the presence of 2 μg/ml doxycycline. Basal expression of Skp2 was highest in LNCaP cells and diminished in DU145 and LNCaP + E6.

After 7 days of exposure to doxycycline, all cell lines reduced expression of Skp2 (Figure 5C, *plus symbols* "+"). LNCaP showed

a marked increase in p27^{Kip1} expression, whereas this relative increase was not as large in cell lines with lower basal Skp2 (Figure 5C). Skp2 down-regulation resulted in reduced proliferation in LNCaP cells. The growth inhibition of Skp2 down-regulation persisted in LNCaP-derived cells even 7 days after doxycycline was removed from the growth medium. No significant effect on proliferation was seen in DU145- and LNCaP + E6–derived cells (both p53 deficient). Skp2 knockdown did not induce other characteristics of senescence in any cell line, including SA-β-gal activity, expression of the SA-β-gal–related protein Glb1, or increased cellular granularity/SSC (not shown). Our results demonstrate that while Skp2 reduction is necessary to mediate TIS and p27^{Kip1} expression, decreased Skp2 activity itself is not sufficient to induce the full senescence phenotype in cancer cells. These results also suggest that cell lines expressing lower basal levels of Skp2 are less responsive to Skp2 down-regulation.

Discussion

In senescence, many studies have addressed the induction and maintenance of senescence in nontransformed cells, either through oncogene-induced senescence or replicative senescence. These tumor suppression processes are frequently disrupted or bypassed in cancer cells. While the idea of TIS as an alternative to cytotoxic treatment strategies was first proposed almost a decade ago [14], a number of recent studies illustrate a quickly growing interest in this topic [13,20,23,24,33,44–46]. However, little is known regarding the regulation of the senescence response in cancer cells.

One obstacle facing senescence research is a lack of specific senescence-inducing compounds. In the current study, we characterized the novel

in vitro and *in vivo* senescence-inducing activity of AZQ, a compound recently identified in a high-throughput senescence screen of small molecules [24]. Although this compound had been previously developed to treat neural and hematological malignancies, limited testing was performed in patients with solid tumors [25]. Moreover, this compound was developed before any awareness of TIS as a tumor response. Our results show that the exposure of a panel of prostate cancer cell lines to 250-nM concentrations of AZQ effectively induces senescence *in vitro*. We also demonstrate that low-dose AZQ administered over extended periods induces senescence with limited apoptosis in prostate tumor xenografts *in vivo*. Tumor growth is significantly inhibited and survival is prolonged. These findings provide initial proof-of-principle for the potential of TIS in cancer treatment and prompt the investigation of other quinone and diaziquone analogs for TIS activity in cancer.
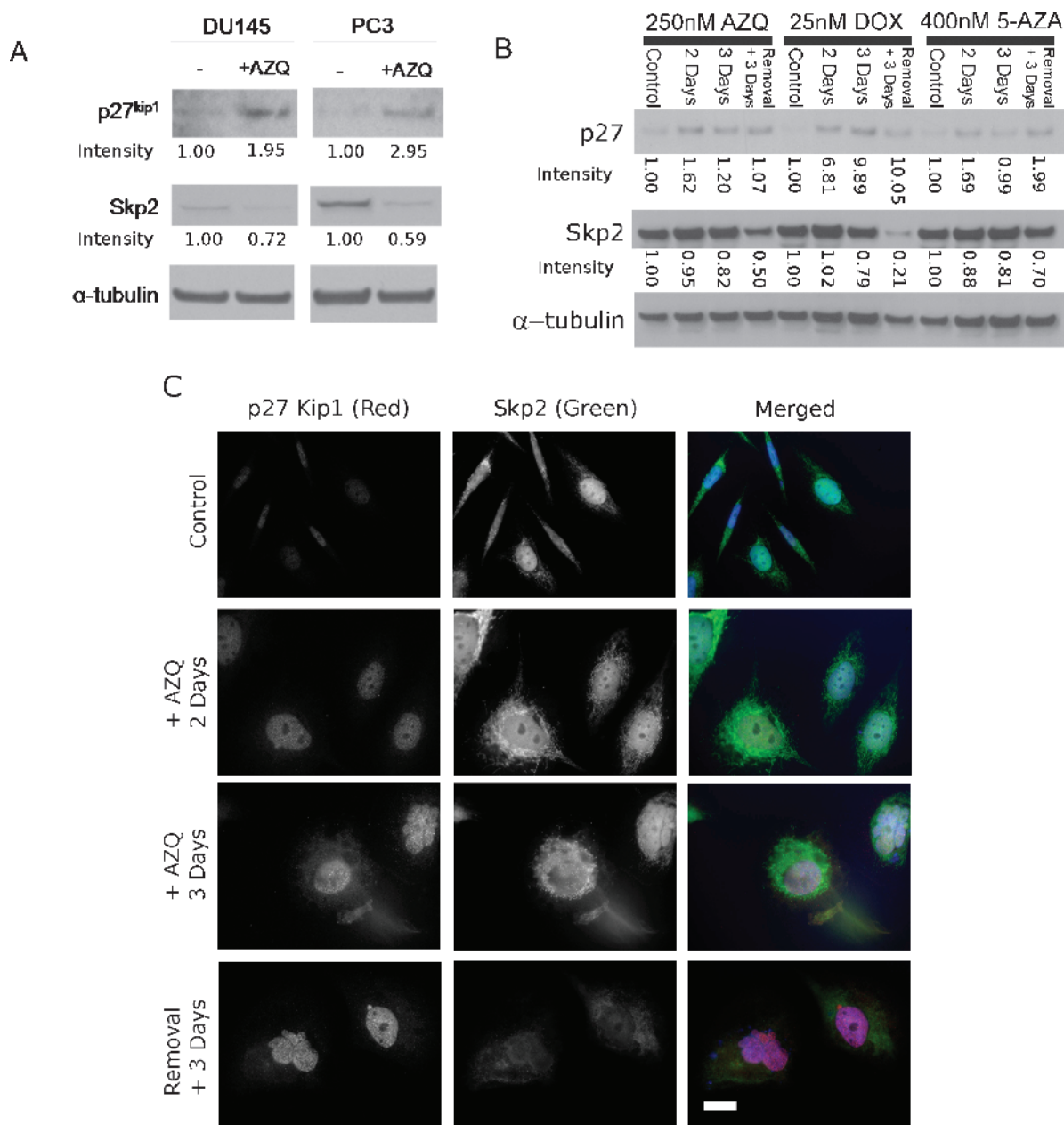

Figure 4. Translocation and decreased expression of Skp2 in senescent prostate cancer cells after treatment with multiple senescence-inducing drugs. Band intensities are normalized to α-tubulin and expressed in relative units. (A) Immunoblot analysis of p27[Kip1] and its relationship to Skp2 in proliferating DU145 and PC3 cells induced to senescence by 250 nM AZQ. Cells were exposed to DMSO (−) or AZQ (+) for 3 days with 3 days of recovery in drug-free medium before harvesting. (B) Time course experiments in PC3 using multiple senescence-inducing agents. Immunoblot analysis of p27[Kip1] and Skp2 expression in untreated PC3 cells (Control) harvested at multiple time points after adding the senescence-inducing drugs AZQ, doxorubicin (DOX), or 5-AZA. Treated PC3 cells were harvested after 2 and 3 days of drug exposure and after 3 days of incubation with drug followed by 3 days in drug-free medium (Removal + 3 Days). p27[Kip1] expression is induced before Skp2 down-regulation with all drugs analyzed. (C) Immunofluorescence microscopy of p27[Kip1] (red) and Skp2 (green) over time during TIS in PC3 cells. Cells were fixed and stained after incubation with AZQ as above. Nuclei were stained with Hoechst 33342 (blue). Scale bar, 20 μm.
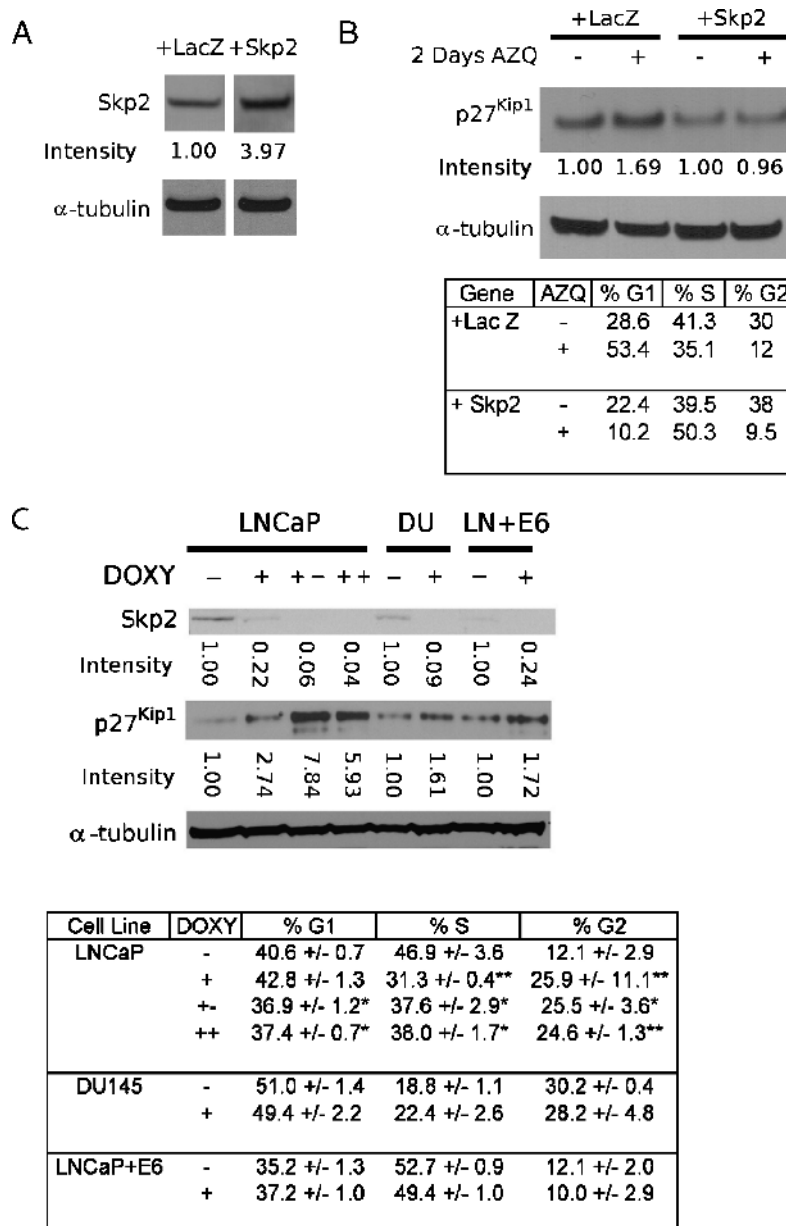
Figure 5. Skp2 is necessary, but not sufficient for TIS. Band intensities are normalized to α-tubulin and expressed in relative units. (A) Over-expression of Skp2 in PC3 cells. PC3 cells were incubated overnight after coelectroporation of GFP with either LacZ or Skp2 expression vectors. Cells were harvested 3 days after electroporation. (B) Overexpression of Skp2 disrupts the senescence response to AZQ. PC3 cells were electroporated, allowed to recover overnight, incubated in drug-free medium (−) or medium + 250 nM AZQ for 2 days, and analyzed for both protein expression and DNA content/cell cycle phase. The overexpression of Skp2 inhibits p27 induction and prevents the decrease in S-phase seen after AZQ treatment. Similar results were demonstrated in DU145 (not shown). (C) Persistent down-regulation of Skp2 expression inhibits proliferation in LNCaP but not DU145 and LNCaP + E6 cells. Skp2-specific shRNAs were expressed in LNCaP, DU145 (DU), and LNCaP + E6 cells (LN + E6). Cells were cultured for 7 days in drug-free medium (−) or with 2 μg/ml doxycycline (DOXY) (+), for 14 days with 2 μg/ml doxycycline (++), or for 7 days with 2 μg/ml doxycycline followed by 7 days in doxycycline-free medium (+−). Parallel samples were analyzed for protein expression and DNA content/cell cycle phase. Skp2 down-regulation inhibits proliferation in LNCaP cells but not DU145 and LNCaP + E6 cells. Student's t test, $*P < .05$, $**P < .01$.

Furthermore, AZQ provides a model compound for the investigation of mechanisms that regulate TIS.

In seeking to define pathways involved in TIS, we screened a panel of CDKIs and found that p27[Kip1] expression increases during TIS in the prostate cancer cell lines investigated. p27[Kip1] has tumor-suppressor functions [47], and its targeted disruption leads to prostatic hyperplasia in mice [48]. In human epithelial cancers, including prostate, p27[Kip1] is commonly downregulated, and this loss of expression correlates with outcome [49]. Disruption through deletion or mutation rarely occurs in human tumors [50,51]. We found that, in the p53-deficient cell lines DU145 and PC3, p27[Kip1] is the only CDKI that is induced. Increased p27[Kip1] expression is a consistent feature of TIS in cancer cells induced through multiple agents and provides a potential marker of this process. Because p16[Ink4a] plays a primary role in the replicative senescence of nontransformed primary prostate epithelia cells [38,41], the expression of p27[Kip1] may represent a

backup mechanism for regulating cell cycle arrest and TIS in transformed cancer cells.

We found that the regulation of p27^{Kip1} in TIS occurs post-translationally and is dependent on Skp2. Recently, Skp2 loss was found to restrict tumorigenesis in *Skp2*$^{-/-}$ *Pten*$^{+/-}$ compound mutants [46]. Our results demonstrate for the first time that Skp2 down-regulation is necessary for TIS. We found that Skp2 expression decreases after TIS induced through a variety of agents (Figure 4*B*). TIS can be stimulated through multiple mechanisms including DNA damage and demethylation [13], induced by doxorubicin and 5-AZA, respectively. Decreased Skp2 is necessary for TIS induced by AZQ because the overexpression of Skp2 blocks growth inhibition after drug exposure in cell lines (Figure 5). Our data suggest that Skp2, a gene frequently upregulated in prostate and other cancers [28], has a major role in the senescence response in cancer cells. Furthermore, up-regulation of Skp2 may be involved in the resistance of senescence induction in cancer cells during treatment.

We also report the novel observation that decreased expression of Skp2 alone does not induce the full senescent phenotype that is observed with AZQ and other agents (Figure 5*C*). The regulation of replicative senescence and oncogene-induced senescence in nontumor cells has been the focus of multiple investigations [42]. However, the regulation of senescence in cancer cells that lack the function of many tumor suppressors is not well defined. The extended down-regulation of Skp2 expression using stable shRNAs was not sufficient to induce senescence in any cell line. Inhibition of proliferation was more significant in LNCaP that expressed higher levels of Skp2 and markedly induced p27^{Kip1}. This lack of effect in other lines may be related to the lower basal expression of Skp2.

The failure of Skp2 to induce senescence suggests that other molecular pathways, possibly upstream of Skp2, are required for the full development of the senescent phenotype by TIS. For instance, the targeting of FOXM1, a transcription factor that regulates expression of Skp2 and other genes, induces senescence in gastric cancer cells [34]. Another potential upstream mediator of TIS is *myc*, whose oncogenic activity induces senescence in nontransformed cells and regulates p27^{Kip1} expression through Skp2 [52,53]. Activities of these transcription factors in addition to Skp2 regulation may prove to be critical for complete senescence induction. In addition, other proteins are also reported to interact with p27^{Kip1} to regulate its stability, including ubiquitin ligases SIAH1/SIP and KPC [54,55]. Recently, MLN4924, a compound that disrupts the activity of multiple ubiquitin ligases in addition to Skp2, was found to induce senescence in PC3 [46]. TIS induction with AZQ, doxorubicin, and 5-AZA down-regulate Skp2 but clearly have the capacity to induce other signals including damage response signal transduction to generate a full senescence response in cancer. Skp2 represents one component of this response, and future study is required to identify other common pathways regulating TIS.

In summary, we conclude that AZQ induces senescence in prostate cancer cells *in vitro* and in xenograft tumors *in vivo*. The drug AZQ provides a benchmark by which future senescence-inducing compounds may be compared both *in vitro* and in tumor models. This drug also presents a tool with which the mechanisms regulating drug-induced senescence and the consequences of this response in tumors may be addressed. Decreased Skp2 and increased p27^{Kip1} are required for TIS induced by multiple drugs. Skp2 and p27^{Kip1} need further investigation as putative markers of the senescence response in treated and untreated tumor tissues. Furthermore, our results suggest that TIS in tumors might be more efficiently achieved by broad stress-inducing agents or by targeting regulators of upstream pathways.

References

[1] Ben-Porath I and Weinberg RA (2004). When cells get stressed: an integrative view of cellular senescence. *J Clin Invest* **113**, 8–13.

[2] Campisi J (2001). Cellular senescence as a tumor-suppressor mechanism. *Trends Cell Biol* **11**, S27–S31.

[3] Campisi J and d'Adda di Fagagna F (2007). Cellular senescence: when bad things happen to good cells. *Nat Rev Mol Cell Biol* **8**, 729–740.

[4] Dimri GP, Lee X, Basile G, Acosta M, Scott G, Roskelley C, Medrano EE, Linskens M, Rubelj I, Pereira-Smith O, et al. (1995). A biomarker that identifies senescent human cells in culture and in aging skin *in vivo*. *Proc Natl Acad Sci USA* **92**, 9363–9367.

[5] d'Adda di Fagagna F (2008). Living on a break: cellular senescence as a DNA-damage response. *Nat Rev Cancer* **8**, 512–522.

[6] Lawless C, Wang C, Jurk D, Merz A, Zglinicki TV, and Passos JF (2010). Quantitative assessment of markers for cell senescence. *Exp Gerontol* **45**, 772–778.

[7] Pospelova TV, Demidenko ZN, Bukreeva EI, Pospelov VA, Gudkov AV, and Blagosklonny MV (2009). Pseudo-DNA damage response in senescent cells. *Cell Cycle* **8**, 4112–4118.

[8] Coppe JP, Patil CK, Rodier F, Sun Y, Munoz DP, Goldstein J, Nelson PS, Desprez PY, and Campisi J (2008). Senescence-associated secretory phenotypes reveal cell-nonautonomous functions of oncogenic *RAS* and the p53 tumor suppressor. *PLoS Biol* **6**, 2853–2868.

[9] Chang BD, Swift ME, Shen M, Fang J, Broude EV, and Roninson IB (2002). Molecular determinants of terminal growth arrest induced in tumor cells by a chemotherapeutic agent. *Proc Natl Acad Sci USA* **99**, 389–394.

[10] Schwarze SR, DePrimo SE, Grabert LM, Fu VX, Brooks JD, and Jarrard DF (2002). Novel pathways associated with bypassing cellular senescence in human prostate epithelial cells. *J Biol Chem* **277**, 14877–14883.

[11] Bringold F and Serrano M (2000). Tumor suppressors and oncogenes in cellular senescence. *Exp Gerontol* **35**, 317–329.

[12] Chang BD, Xuan Y, Broude EV, Zhu H, Schott B, Fang J, and Roninson IB (1999). Role of p53 and p21$^{waf1/cip1}$ in senescence-like terminal proliferation arrest induced in human tumor cells by chemotherapeutic drugs. *Oncogene* **18**, 4808–4818.

[13] Ewald JA, Desotelle JA, Wilding G, and Jarrard DF (2010). Therapy-induced senescence in cancer. *J Natl Cancer Inst* **102**, 1536–1546.

[14] Roninson IB (2003). Tumor cell senescence in cancer treatment. *Cancer Res* **63**, 2705–2715.

[15] Chang BD, Broude EV, Dokmanovic M, Zhu H, Ruth A, Xuan Y, Kandel ES, Lausch E, Christov K, and Roninson IB (1999). A senescence-like phenotype distinguishes tumor cells that undergo terminal proliferation arrest after exposure to anticancer agents. *Cancer Res* **59**, 3761–3767.

[16] Schwarze SR, Fu VX, Desotelle JA, Kenowski ML, and Jarrard DF (2005). The identification of senescence-specific genes during the induction of senescence in prostate cancer cells. *Neoplasia* **7**, 816–823.

[17] Roberson RS, Kussick SJ, Vallieres E, Chen SY, and Wu DY (2005). Escape from therapy-induced accelerated cellular senescence in p53-null lung cancer cells and in human lung cancers. *Cancer Res* **65**, 2795–2803.

[18] te Poele RH, Okorokov AL, Jardine L, Cummings J, and Joel SP (2002). DNA damage is able to induce senescence in tumor cells *in vitro* and *in vivo*. *Cancer Res* **62**, 1876–1883.

[19] Di X, Bright AT, Bellott R, Gaskins E, Robert J, Holt S, Gewirtz D, and Elmore L (2008). A chemotherapy-associated senescence bystander effect in breast cancer cells. *Cancer Biol Ther* **7**, 864–872.

[20] Ewald JA, Desotelle JA, Almassi N, and Jarrard DF (2008). Drug-induced senescence bystander proliferation in prostate cancer cells *in vitro* and *in vivo*. *Br J Cancer* **98**, 1244–1249.

[21] Schmitt CA, Fridman JS, Yang M, Lee S, Baranov E, Hoffman RM, and Lowe SW (2002). A senescence program controlled by p53 and p16[INK4a] contributes to the outcome of cancer therapy. *Cell* **109**, 335–346.

[22] Xue W, Zender L, Miething C, Dickins RA, Hernando E, Krizhanovsky V, Cordon-Cardo C, and Lowe SW (2007). Senescence and tumour clearance is triggered by p53 restoration in murine liver carcinomas. *Nature* **445**, 656–660.

[23] Haugstetter AM, Loddenkemper C, Lenze D, Grone J, Standfuss C, Petersen I, Dorken B, and Schmitt CA (2010). Cellular senescence predicts treatment outcome in metastasised colorectal cancer. *Br J Cancer* **103**, 505–509.

[24] Ewald JA, Peters N, Desotelle JA, Hoffmann FM, and Jarrard DF (2009). A high-throughput method to identify novel senescence-inducing compounds. *J Biomol Screen* **14**, 853–858.

[25] Bender JF, Grillo-Lopez AJ, and Posada JG Jr (1983). Diaziquone (AZQ). *Invest New Drugs* **1**, 71–84.

[26] Majumder PK, Grisanzio C, O'Connell F, Barry M, Brito JM, Xu Q, Guney I, Berger R, Herman P, Bikoff R, et al. (2008). A prostatic intraepithelial neoplasia–dependent p27[Kip1] checkpoint induces senescence and inhibits cell proliferation and cancer progression. *Cancer Cell* **14**, 146–155.

[27] Frescas D and Pagano M (2008). Deregulated proteolysis by the F-box proteins SKP2 and β-TrCP: tipping the scales of cancer. *Nat Rev Cancer* **8**, 438–449.

[28] Hershko DD (2008). Oncogenic properties and prognostic implications of the ubiquitin ligase Skp2 in cancer. *Cancer* **112**, 1415–1424.

[29] Loda M (2000). p27[KIP1]: androgen regulation and prognostic significance in prostate cancer. *Adv Clin Path* **4**, 226–232.

[30] Waltregny D, Leav I, Signoretti S, Soung P, Lin D, Merk F, Adams JY, Bhattacharya N, Cirenei N, and Loda M (2001). Androgen-driven prostate epithelial cell proliferation and differentiation *in vivo* involve the regulation of p27. *Mol Endocrinol* **15**, 765–782.

[31] Gao D, Inuzuka H, Tseng A, and Wei W (2009). Akt finds its new path to regulate cell cycle through modulating Skp2 activity and its destruction by APC/Cdh1. *Cell Div* **4**, 11.

[32] Majumder PK and Sellers WR (2005). Akt-regulated pathways in prostate cancer. *Oncogene* **24**, 7465–7474.

[33] Lin HK, Wang G, Chen Z, Teruya-Feldstein J, Liu Y, Chan CH, Yang WL, Erdjument-Bromage H, Nakayama KI, Nimer S, et al. (2009). Phosphorylation-dependent regulation of cytosolic localization and oncogenic function of Skp2 by Akt/PKB. *Nat Cell Biol* **11**, 420–432.

[34] Zeng J, Wang L, Li Q, Li W, Bjorkholm M, Jia J, and Xu D (2009). FoxM1 is up-regulated in gastric cancer and its inhibition leads to cellular senescence, partially dependent on p27[kip1]. *J Pathol* **218**, 419–427.

[35] Westbrook L, Ramanathan HN, Isayeva T, Mittal AR, Qu Z, Johnson MD, Kern FG, Ponnazhagan S, Grubbs CJ, and Thottassery JV (2009). High Cks1 expression in transgenic and carcinogen-initiated mammary tumors is not always accompanied by reduction in p27[Kip1]. *Int J Oncol* **34**, 1425–1431.

[36] Ewald JA, Wilkinson JC, Guyer CA, and Staros JV (2003). Ligand- and kinase activity–independent cell survival mediated by the epidermal growth factor receptor expressed in 32D cells. *Exp Cell Res* **282**, 121–131.

[37] Passaniti A, Adler SH, and Martin GR (1992). New models to define factors determining the growth and spread of human prostate cancer. *Exp Gerontol* **27**, 559–566.

[38] Schwarze SR, Shi Y, Fu VX, Watson PA, and Jarrard DF (2001). Role of cyclin-dependent kinase inhibitors in the growth arrest at senescence in human prostate epithelial and uroepithelial cells. *Oncogene* **20**, 8184–8192.

[39] Fu VX, Schwarze SR, Kenowski ML, Leblanc S, Svaren J, and Jarrard DF (2004). A loss of insulin-like growth factor-2 imprinting is modulated by CCCTC-binding factor down-regulation at senescence in human epithelial cells. *J Biol Chem* **279**, 52218–52226.

[40] Liliensiek SJ, Schell K, Howard E, Nealey P, and Murphy CJ (2006). Cell sorting but not serum starvation is effective for SV40 human corneal epithelial cell cycle synchronization. *Exp Eye Res* **83**, 61–68.

[41] Jarrard DF, Sarkar S, Shi Y, Yeager TR, Magrane G, Kinoshita H, Nassif N, Meisner L, Newton MA, Waldman FM, et al. (1999). p16/pRb pathway alterations are required for bypassing senescence in human prostate epithelial cells. *Cancer Res* **59**, 2957–2964.

[42] Campisi J (2005). Senescent cells, tumor suppression, and organismal aging: good citizens, bad neighbors. *Cell* **120**, 513–522.

[43] Ben-Porath I and Weinberg RA (2005). The signals and pathways activating cellular senescence. *Int J Biochem Cell Biol* **37**, 961–976.

[44] Alimonti A, Nardella C, Chen Z, Clohessy JG, Carracedo A, Trotman LC, Cheng K, Varmeh S, Kozma SC, Thomas G, et al. (2010). A novel type of cellular senescence that can be enhanced in mouse models and human tumor xenografts to suppress prostate tumorigenesis. *J Clin Invest* **120**, 681–693.

[45] Huck JJ, Zhang M, McDonald A, Bowman D, Hoar KM, Stringer B, Ecsedy J, Manfredi MG, and Hyer ML (2010). MLN8054, an inhibitor of Aurora A kinase, induces senescence in human tumor cells both *in vitro* and *in vivo*. *Mol Cancer Res* **8**, 373–384.

[46] Lin HK, Chen Z, Wang G, Nardella C, Lee SW, Chan CH, Yang WL, Wang J, Egia A, Nakayama KI, et al. (2010). Skp2 targeting suppresses tumorigenesis by Arf-p53–independent cellular senescence. *Nature* **464**, 374–379.

[47] Chu IM, Hengst L, and Slingerland JM (2008). The Cdk inhibitor p27 in human cancer: prognostic potential and relevance to anticancer therapy. *Nat Rev Cancer* **8**, 253–267.

[48] Cordon-Cardo C, Koff A, Drobnjak M, Capodieci P, Osman I, Millard SS, Gaudin PB, Fazzari M, Zhang ZF, Massague J, et al. (1998). Distinct altered patterns of p27[KIP1] gene expression in benign prostatic hyperplasia and prostatic carcinoma. *J Natl Cancer Inst* **90**, 1284–1291.

[49] Hershko DD (2010). Cyclin-dependent kinase inhibitor p27 as a prognostic biomarker and potential cancer therapeutic target. *Future Oncol* **6**, 1837–1847.

[50] Kawamata N, Morosetti R, Miller CW, Park D, Spirin KS, Nakamaki T, Takeuchi S, Hatta Y, Simpson J, Wilczynski S, et al. (1995). Molecular analysis of the cyclin-dependent kinase inhibitor gene p27/Kip1 in human malignancies. *Cancer Res* **55**, 2266–2269.

[51] Ponce-Castaneda MV, Lee MH, Latres E, Polyak K, Lacombe L, Montgomery K, Mathew S, Krauter K, Sheinfeld J, Massague J, et al. (1995). p27[Kip1]: chromosomal mapping to 12p12-12p13.1 and absence of mutations in human tumors. *Cancer Res* **55**, 1211–1214.

[52] Campaner S, Doni M, Hydbring P, Verrecchia A, Bianchi L, Sardella D, Schleker T, Perna D, Tronnersjo S, Murga M, et al. (2010). Cdk2 suppresses cellular senescence induced by the c-*myc* oncogene. *Nat Cell Biol* **12**, 54–59, sup pp. 51–14.

[53] Bretones G, Acosta JC, Caraballo JM, Ferrandiz N, Gomez-Casares MT, Albajar M, Blanco R, Ruiz P, Hung WC, Albero MP, et al. (2011). *SKP2* oncogene is a direct *MYC* target gene and MYC down-regulates p27[KIP1] through SKP2 in human leukemia cells. *J Biol Chem* **286**, 9815–9825.

[54] Kamura T, Hara T, Matsumoto M, Ishida N, Okumura F, Hatakeyama S, Yoshida M, Nakayama K, and Nakayama KI (2004). Cytoplasmic ubiquitin ligase KPC regulates proteolysis of p27(Kip1) at G₁ phase. *Nat Cell Biol* **6**, 1229–1235.

[55] Nagano Y, Fukushima T, Okemoto K, Tanaka K, Bowtell D, Ronai Z, Reed J, and Matsuzawa S (2011). SIAH1/SIP regulates p27[Kip1] stability and cell migration under metabolic stress. *Cell Cycle* **10**, 2592–2602.